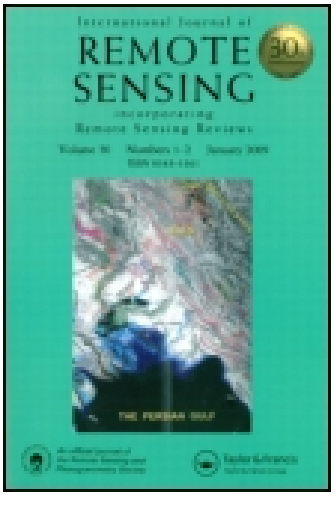

International Journal of Remote Sensing
Publication details, including instructions for authors and subscription information:
http://www.tandfonline.com/loi/tres20

Particulate organic carbon in the surface waters of the North Atlantic: spatial and temporal variability based on satellite ocean colour

Malgorzata Stramska[ab]
[a] Institute of Oceanology of the Polish Academy of Sciences, 81-712 Sopot, Poland
[b] Department of Earth Sciences, Szczecin University, Szczecin 70-383, Poland
Published online: 25 Jul 2014.

To cite this article: Malgorzata Stramska (2014) Particulate organic carbon in the surface waters of the North Atlantic: spatial and temporal variability based on satellite ocean colour, International Journal of Remote Sensing, 35:13, 4717-4738

To link to this article: http://dx.doi.org/10.1080/01431161.2014.919686

International Journal of Remote Sensing, 2014
Vol. 35, No. 13, 4717–4738, http://dx.doi.org/10.1080/01431161.2014.919686

Taylor & Francis
Taylor & Francis Group

Particulate organic carbon in the surface waters of the North Atlantic: spatial and temporal variability based on satellite ocean colour

Malgorzata Stramska[a,b]*

[a]*Institute of Oceanology of the Polish Academy of Sciences, 81-712 Sopot, Poland;* [b]*Department of Earth Sciences, Szczecin University, Szczecin 70-383, Poland*

(*Received 20 January 2014; accepted 31 March 2014*)

We have examined the 16-year time series of particulate organic carbon (POC) concentration in the surface waters of the North Atlantic derived from SeaWiFS and MODIS-Aqua data. The annual mean POC concentrations are the highest in the northern North Atlantic, reaching 120 mg m^{-3}. Moving south, the mean annual POC concentrations decrease to minimum values of about 30 mg m^{-3} at around 30° N and increase in the equatorial region to about 70 mg m^{-3}. The seasonal amplitude of POC concentration in the northern North Atlantic region is larger when compared to other regions. The annual mean surface POC concentrations in the entire North Atlantic basin show a statistically significant trend with an average decrease of 0.79 mg m^{-3} $year^{-1}$. Regionally averaged 16-year mean POC biomass integrated over the optical depth, euphotic depth, and mixed-layer depth is estimated at about 1.27, 4.34, and 4.59 g m^{-2}, respectively. Even larger biomass of 6.26 g m^{-2} is estimated if one chooses to use in the calculations the greatest from the daily values of the estimates listed above at each pixel of the satellite data. Comparisons of POC biomass with primary productivity allowed us to assess temporal and spatial patterns of POC losses.

1. Introduction

An improved knowledge of the particulate organic carbon (POC) reservoir is of interest to research on ocean biogeochemical cycles, ocean ecosystems, and climate studies relating to the ocean carbon cycle (e.g. Houghton 2007). With recent development of POC algorithms (Stramski et al. 2008), satellite ocean colour observations can greatly advance our understanding of these issues by providing simultaneous POC data for large areas of the ocean and long-term monitoring.

Traditionally, ocean colour has supplied estimates of surface chlorophyll-*a* concentration, Chl (Clarke, Ewing, and Lorenzen 1970; Gordon and Morel 1983; McClain, Feldman, and Hooker 2004). However, of particular interest to ocean biogeochemistry and its role in climate change is not Chl, but carbon. Attempts have been made to estimate POC from remotely sensed Chl. However, such estimates are not very accurate because, even in Case I waters (Morel and Prieur 1977), the bulk carbon to chlorophyll ratio can vary 10 fold or more on a global scale (Morel 1988). Therefore, it is more practical to use algorithms specifically designed for the direct assessment of POC from ocean colour.

A rigorous remote-sensing capability for estimating POC needs to be based on the knowledge about the relationships between POC and the spectral remote-sensing reflectance, $R_{rs}(\lambda)$ (or a combination of R_{rs} and inherent optical properties, IOPs, data). Recently published POC algorithms (Stramski et al. 2008) satisfy that requirement and POC

*Email: mstramska@wp.pl

estimates obtained through these algorithms have been used in this study. These algorithms were derived on simultaneous *in situ* measurements of $R_{rs}(\lambda)$ and a collection of water samples for POC determinations, in a similar manner as was performed by the ocean colour community to construct ocean colour Chl algorithms (O'Reilly et al. 1998, 2000). The work of Stramski et al. (2008) covered a broad range of oceanic conditions, from hyper-oligotrophic and oligotrophic waters within subtropical gyres to eutrophic coastal upwelling regimes. This suggests that such algorithms should perform well in different bio-optical provinces of the ocean. Note that to date only a few attempts have been made in which simultaneously collected *in situ* data were used for the development of empirical algorithms for estimating POC (Stramski et al. 1999; Stramska and Stramski 2005a; Pabi and Arrigo 2006; Stramski et al. 2008; Son et al. 2009; Allison, Stramski, and Mitchell 2010). Alternative approaches have also been applied; however, algorithms based on POC and optical data that were not all collected *in situ*, or were not collected during the same field experiment (Loisel et al. 2001, 2002; Mishonov, Gardner, and Richardson 2003; Gardner, Mishonov, and Richardson 2006), might have more significant limitations than the algorithms of Stramski et al. (2008).

In this article, the 16-year time series of POC concentrations in the North Atlantic derived from data collected by the Sea-viewing Wide Field-of-view Sensor (SeaWiFS) aboard the OrbView-2 satellite and the Moderate Resolution Imaging Spectroradiometer deployed on the Aqua (EOS PM) satellite (MODIS-A) have been analysed. Similar analyses have been attempted before (Gardner, Mishonov, and Richardson 2006; Stramska 2009; Duforêt-Gaurier et al. 2010) but they were based on significantly shorter time series of the ocean colour data (10 years or less). In this article, we focus our interest on the North Atlantic, because it is a region where phytoplankton blooms have been traditionally attributed an important role in the ocean carbon cycle (Longhurst and Harrison 1989; Legendre et al. 1993). In particular, in the northern North Atlantic, the biological carbon pump can be quite effective, because biological processes are characterized by high seasonal amplitudes of productivity, phytoplankton blooms are not matched by concurrent secondary production, and deep-water formation is active (Aagaard, Swift, and Carmack 1985). Deep-water formation processes provide the link between the northern North Atlantic carbon export and the rest of the global oceanic waters through the deep ocean 'conveyor belt'. It has been estimated that dissolved organic carbon (DOC) export contributes less than 20% of the total export production within the North Atlantic (Carlson et al. 2010); therefore, export of particulate matter is significant. There are however large latitudinal differences. On the basin scale, the availability of inorganic nutrients exerts a major control on phytoplankton biomass, primary productivity (PP), community structure, and POC export, which results in prominent latitudinal gradients in the North Atlantic (Longhurst 1998; Dutkiewicz et al. 2001). Typically, high latitude and temperate systems receive substantial amounts of nutrients from deep waters via vertical mixing. In contrast, phytoplankton communities inhabiting low-latitude environments, such as stratified, subtropical gyres, largely rely on local recycling and diapycnal nutrient fluxes to sustain their standing stocks. Phytoplankton growth involves a balance between nutrient and light supply. Thus, the dominant scheme in the North Atlantic is a transition from a high-latitude system where phytoplankton blooms are triggered by increasing light availability and water column stability in spring, to a low-latitude system where they are associated with a decrease of vertical stability when nutrients from deep waters can fuel the permanently warm and nutrient-exhausted mixed layer (ML). The interplay between these two competing effects has been discussed since the publication of Sverdrup's (1953) critical depth theory and Menzel and Ryther's (1961) observations of phytoplankton

blooms in the Sargasso Sea. Sverdrup's critical depth theory has been known to have some conceptual value and not to explain all the details of interactions involved in phytoplankton bloom development, as it has been well documented that the blooms can start before the onset of seasonal stratification (e.g. Townsend et al. 1992; Stramska and Dickey 1993, 1994). These issues have been recently discussed in depth by Behrenfeld (2010) and Behrenfeld and Boss (2014).

Although considerable literature is available on the development of phytoplankton blooms in the North Atlantic, spatial distributions of POC reservoirs and their variability are not documented as well. Thus, the main goals of this article are to quantify surface POC concentrations in different regions of the North Atlantic, to discuss regional variability of the POC biomass contained in the oceanic surface layer, and to compare these estimates with regional estimates of PP.

2. Data sources and methods

2.1. POC data

This study is based on ocean surface POC concentrations derived from data collected by SeaWiFS and MODIS-Aqua (Franz et al. 2007). Each of these ocean colour missions provided global coverage of remote-sensing reflectances at selected spectral bands in the visible and near-infrared spectral regions approximately every two days. The standard data processing procedures applied by NASA include atmospheric corrections and removal of pixels with land, ice, cloud, or heavy aerosol load. As a result the retrievals of the ocean remote-sensing reflectance have uncertainties of ~3% (O'Reilly et al. 1998, 2000). For our study, we used Level 3 POC data (Standard Mapped Images with a nominal 9.2 km resolution at the equator, reprocessing versions R2010.0 and R2013.1 of SeaWiFS and MODIS-A data, respectively). The POC data product provided by NASA is based on the Stramski et al. (2008) algorithm. Note that similar to satellite-derived Chl, POC data represent concentrations just below the water surface (see also Stramska and Stramski 2005b).

Because the POC algorithms are non-linear, we have attempted to minimize the biases, which could be accrued if our calculations were completed on temporal averages (such as monthly composites) of satellite data. Therefore, we started our calculations with daily fields of POC concentrations. The original set of daily POC concentrations (mg m^{-3}) includes 13 years (1998–2010) of SeaWiFS data and 11 years (2002–2013) of MODIS-A data. SeaWiFS data in 2008–2010 have extensive time periods with missing data; therefore, we have decided to not use SeaWiFS data from 2008 to 2010. From the rest of daily POC imagery, the 21-day moving averages were calculated to fill in the missing data. Next, we have calculated monthly and annual averages, and the 16-year averaged POC concentrations, which are presented in Figure 1. For our approach of contrasting regional POC reservoirs, we have defined four study regions. Geographical boundaries for these regions were subjectively chosen based on the large-scale POC patterns displayed in Figure 1. These regions include: region 1 – northern North Atlantic (60–46.7° N, 47–15° W); region 2 – temperate zone (44–30° N, 58.4–16° W); region 3 – oligotrophic region (30–15 °N, 63.3–34.2° W); and region 4 – equatorial Atlantic (23.3° N–1.6° S, 34.2–18.3° W). When we refer to the North Atlantic region, we have in mind the area extending from 70° N to 10° S as shown in Figure 1 (i.e. excluding the inland seas such as the Mediterranean, Black and Baltic Seas, and the Gulf of Mexico). This choice of the boundaries for the basin-scale POC estimates has been motivated by the fact that we

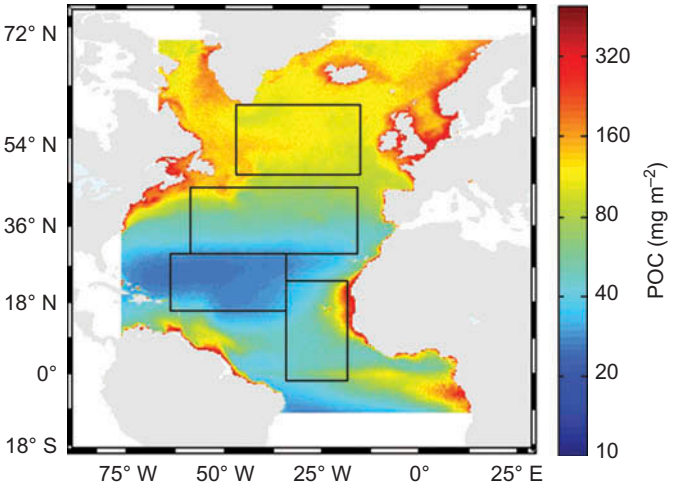

Figure 1. The 16-year averaged (1997–2013) surface POC concentrations in the North Atlantic derived from SeaWiFS and MODIS-A data. The area of the North Atlantic region where ocean colour data were analysed extends from 70° N to 10° S (inland seas are excluded) and is shown in colours. Additionally, four study regions are indicated by black boxes.

wanted to exclude the polar region north of 70° N (because of the problem of missing data) and we intended to include in our analysis the area of the equatorial upwelling, extending south of the equator.

Time series were constructed by calculating the weighted averages from all pixels within each region. The weighted average takes into account that pixel area at a given latitude is equal to the cosine of this latitude multiplied by the pixel area at the equator. This regional averaging provides POC estimates representative of mean conditions over relatively large sections of the ocean, removes the small and mesoscale features, and reduces (but does not eliminate) gaps in the time series due to missing data. Gaps are still present after this spatial averaging in the northern region in winter. These gaps are left unfilled in the figures presented below. In our estimates of the annual mean POC concentrations, these gaps were filled by linear interpolation. In the final time series presented below, data in years 2003–2007 represent average POC concentrations from SeaWiFS and MODIS-A observations. Comparisons of the POC estimates obtained in these years by both radiometers shows a good agreement (Figure 2). The POC estimates for years 1997–2002 are based on SeaWiFS data, whereas for years 2008–2013 they are based on MODIS-A data. Using these time series data we calculated POC anomalies, as the difference between POC concentration observed on a given day of the year and the 16-year averaged POC concentration for the same day number. All these calculations were carried out for our four study regions and for the North Atlantic, as shown in Figure 1.

2.2. *POC reservoirs and other data*

One of the biggest challenges in modern oceanography is the need to estimate reservoirs of organic matter in the ocean. The methods used to derive our estimates of the POC reservoirs in the surface waters in the North Atlantic are described in this section.

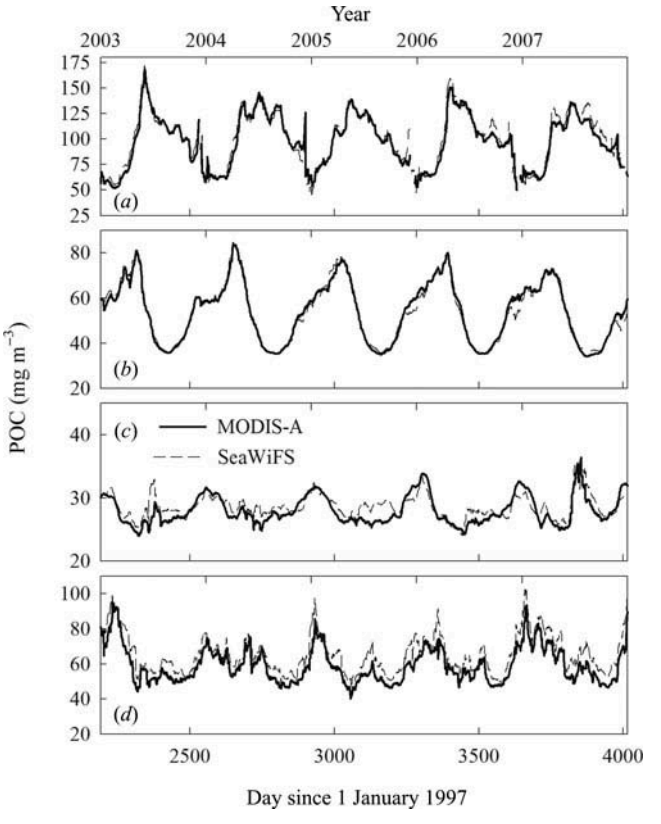

Figure 2. Comparison of SeaWiFS and MODIS-A time series of regionally averaged POC concentrations in the four study regions in the years 2003–2007. Panels (*a*), (*b*), (*c*), and (*d*) correspond to regions 1, 2, 3, and 4, respectively (see explanation in the text).

As discussed in Stramska (2009), the meaning of the oceanic surface layer is rather broad and needs to be defined more precisely if we are to discuss the POC reservoirs in a quantitative sense. For example, oceanic surface layer can be understood as the optical depth (z_{90}), the euphotic depth (z_{eu}), or the mixed layer depth (MLD). The ML of the ocean is the layer near the ocean surface with vertically quasi-homogeneous water properties (temperature, salinity, density; Niiler and Kraus 1977; Kraus, Bleck, and Hanson 1988; Lorbacher et al. 2006). The intense vertical turbulent mixing near the surface is the cause of the observed vertical uniformity. The ML concept has been used by Stramska (2009) to estimate the POC reservoirs in the oceanic surface waters by assuming that the POC concentration within the ML is nearly homogenous and that the POC integrated over the ML (POC_{MLD}) can be simply calculated as $POC_{MLD} = POC \cdot MLD$. In another approach, POC reservoirs can be assessed in the oceanic surface layer defined as the euphotic depth. The euphotic depth limits the surface layer of the water, where there is sufficient light to support PP and is defined as the depth where photosynthetic available radiation (PAR) is 1% of its surface value.

In the current article, the surface POC concentrations were converted to POC biomass through the relationships derived from observational data. Towards this objective, we investigated the historical *in situ* data obtained from the Joint Global Ocean Flux Study

(JGOFS) website (usjgofs.whoi.edu/jg/dir/jgofs/). For our goal we selected these data sets, which included simultaneous information about z_{eu}, MLD, vertical profiles of beam attenuation coefficient at 660 nm (c_{p660}), and POC concentrations estimated from water samples collected at selected water depths. For each station, the local relationship between c_{p660} and POC concentration was estimated. Three examples of such relationships are shown in Figure 3 (panels on the left side of the figure). Based on the station-specific relationships, vertical profiles of c_{p660} measured at each station were converted to the vertical profiles of POC concentration (plots on the right side of Figure 3). In the final step, POC concentrations were averaged over the MLD and z_{eu}. In this way we analysed data from 102 stations from the Arabian Sea, Southern Ocean, Equatorial Pacific, and Bermuda Atlantic Time-Series experiments. Because of limited availability of data sets with all the required parameters, we had to include in our analysis data not only from the North Atlantic but also from other geographic regions, in order to obtain a sufficient

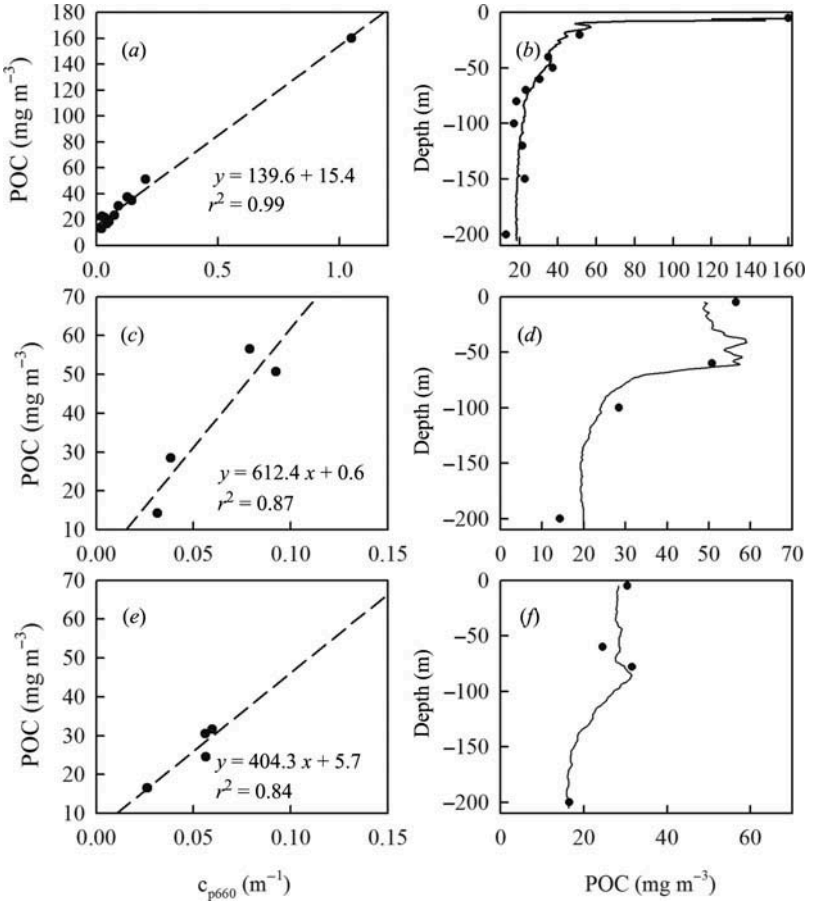

Figure 3. Plots (*a*), (*c*), (*e*). Example relationships between beam attenuation coefficient at 660 nm (c_{p660}) and POC concentrations determined from water samples at three stations: (*a*) 2.1° N, 141.4° W; 26 August 1992; (*c*) 7.0° N, 17.5° W; 3 November 2005; and (*e*) 33.5° N, 14.5° W; 27 October 2005. Plots (*b*), (*d*), and (*e*). Vertical profiles of POC concentration determined from measured vertical profiles of c_{p660} and the relationships between c_{p660} and POC concentrations (shown in (*a*), (*c*), and (*e*)).

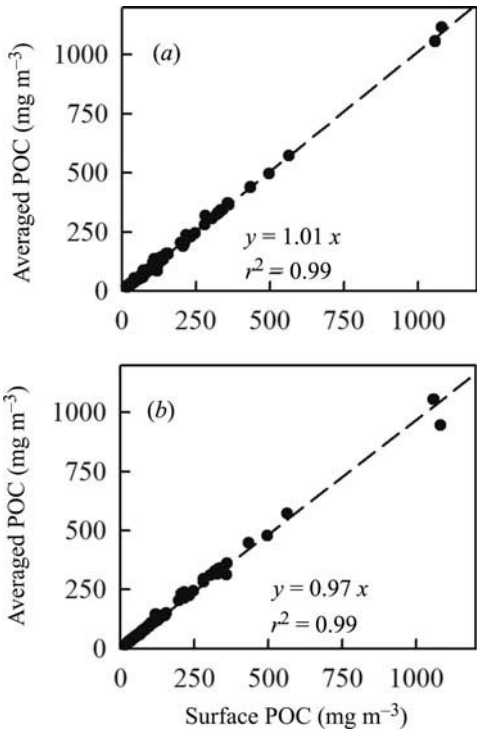

Figure 4. (*a*) POC concentration averaged over the euphotic depth as a function of surface POC concentration. (*b*) POC concentration averaged over the MLD as a function of surface POC concentration (data from 102 *in situ* stations).

number of data points. As a result from this analysis, the relationships between surface POC concentration and POC concentration averaged over the MLD and z_{eu} have been derived (Figure 4). These relationships were subsequently used to convert the surface POC concentrations determined from satellite data to POC reservoirs present in the surface waters of the ocean. To calculate POC_{MLD}, we used the MLD estimates derived from ocean models for the same day and geographical location as the satellite POC determinations (MLD data available at web.science.oregonstate.edu/ocean.productivity/site.php, Behrenfeld et al. 2005; Westberry et al. 2008). We also used the z_{eu} estimates provided by the NASA OceanColor website (oceancolor.gsfc.nasa.gov) as the euphotic depth product (Zeu_lee, Lee et al. 2007) to calculate POC integrated over the euphotic depth (POC_{zeu}).

Another estimate of POC reservoir has been based on the concept of optical depth (z_{90}). Gordon and McCluney (1975) showed that 90% of all the remotely sensed ocean colour radiance originates from z_{90}. The concept of optical depth has been used before to estimate POC biomass in oceanic surface waters (Gardner, Mishonov, and Richardson 2006; Stramska 2009; Duforêt-Gaurier et al. 2010). In these calculations, z_{90} was estimated using the SeaWiFS-derived diffuse attenuation coefficient data product (K_{490}) and the relationship $z_{90} = 1/K_{490}$. The POC content integrated over one attenuation depth (POC_{opt}) was then calculated as $POC_{opt} = POC/K_{490}$ (see also Campbell, Blaisdell, and Darzi 1995). In this article, we carried out similar calculations to compare our new estimates of POC biomass with the earlier estimates. In our calculations we used the

NASA Kd_Lee(490) product, which has been validated in a wide range of oceanic and coastal conditions including case 1 and case 2 waters (Lee, Du, and Arnone 2005, Lee, Darecki et al. 2005, 2007; Doron et al. 2007).

The PP data used in this article represent PP estimates distributed through the Ocean Productivity Web Page (www.science.oregonstate.edu/ocean.productivity/) and include data from the Vertically Generalized Production Model, VGPM (Behrenfeld and Falkowski 1997), the Eppley-VGPM version of the model, and the Carbon-based Production Model, CBPM (Behrenfeld et al. 2005; Westberry et al. 2008).

3. Results and discussion

3.1. POC concentrations

Spatial distribution of the 16-year averaged surface POC concentration in the North Atlantic is presented in Figure 1. Recall that the spatial distribution of the surface POC concentration in the ocean is, in general, governed by both the biological processes (primary production and recycling) and the physical processes (vertical mixing and advection). The significance of the different processes can vary in time and space. The large-scale patterns in POC concentration shown in Figure 1 are similar to the large-scale distribution of Chl (not shown), because phytoplankton production is a primary source of POC particles in the open ocean surface waters (e.g. Siegel et al. 2013; Yoder and Kennelly 2006).

The concentrations of POC are high in the northern North Atlantic waters due to the intense phytoplankton blooms of the spring and summer. Elevated POC concentrations are also present in the equatorial upwelling zone due to favourable growth conditions for phytoplankton. These conditions are caused by trade winds and the divergence of water transport and upwelling along the equator, which brings up nutrient-rich and cool water that nourishes phytoplankton (e.g. Siegel et al. 2013; Yoder and Kennelly 2006). In contrast, open-ocean mid-latitude regions, such as the region east of Florida, typically have low POC concentrations, because these mid-latitude regions are a significant distance away from the source of nutrients and runoff from land. In addition, these are regions of convergence and downwelling of surface water masses and thus PP is low (Westberry et al. 2008). Figure 2 compares the time series of POC concentration in our four study regions as estimated with SeaWiFS and MODIS-A observations, and documents good agreement between both sensors. Figure 2 also demonstrates the seasonal variability of POC in the North Atlantic, which is closely linked to seasonal phytoplankton blooms. These blooms start around February–March at the latitude of the Sargasso Sea and can be seen in the true ocean colour images (not shown here) as a green colour moving with time gradually north until they reach the latitude of Spitsbergen. Accordingly, the POC concentrations are low during January and February, when the values of spatially averaged POC concentrations in the northern North Atlantic (Figures 2 (*a*) and (*b*)) range from about 60 to 80 mg m^{-3}. By June, POC concentrations in the northern North Atlantic are often greater than 120 mg m^{-3}. At the same time, low POC concentrations (30 mg m^{-3} and less) in the mid-latitude region (Figure 2(*c*)) seem to be quite stable throughout the year.

To illustrate the major patterns in temporal and spatial variability of POC in the North Atlantic, we plotted in Figure 5 the annual cycles of POC concentration. These data represent spatial averages (in the four geographical regions defined in Section 2.1) plotted as a function of the day of the year. Note that there is relatively little variability in the

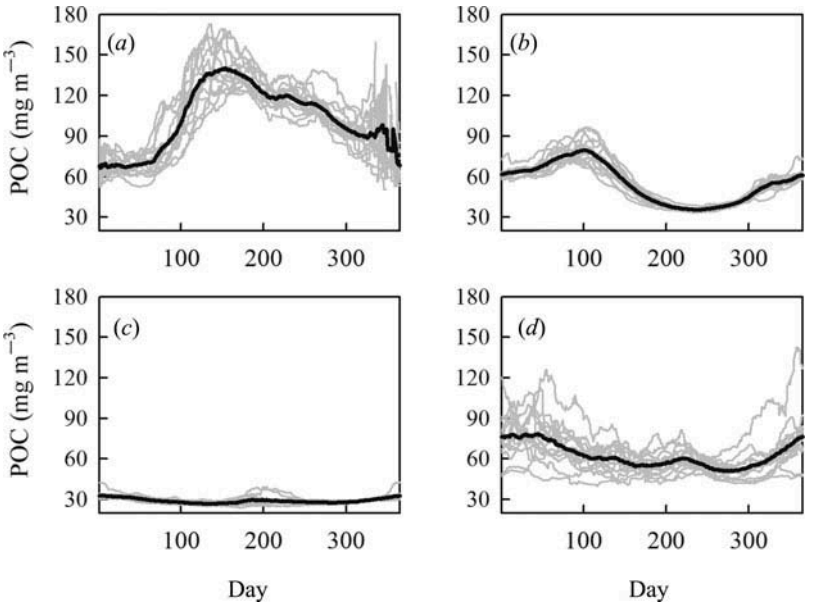

Figure 5. Annual (1998–2012) time series (grey lines) and the 16-year averaged annual cycle (black line) of spatially averaged surface POC concentration in the four study regions. Panels (*a*), (*b*), (*c*), and (*d*) correspond to regions 1, 2, 3, and 4, respectively.

seasonal POC patterns between different years for each of the regions. The highest POC concentrations are observed during spring/summer in the northern region (Figure 5(*a*)), whereas the lowest are observed in the oligotrophic region (Figure 5(*c*)). Note also the differences between regions. The spring increase in the POC concentration is observed somewhat earlier in the temperate region (see Figures 2(*b*) and 5(*b*)) than in the northern region (Figures 2(*a*) and 5(*a*)), whereas in the oligotrophic region (Figure 5(*c*)) the seasonal changes have small amplitude and POC concentrations are generally low through the year.

In Figure 6 the same data are shown as the time series of POC anomalies (calculated as the difference between POC concentration recorded on a given day and the 16-year averaged POC concentration for the same day number). The anomalies allow us to highlight inter-annual variability. The data shown in Figure 6 indicate that the POC anomalies are within ±30 mg m^{-3}. The absolute values of the POC anomalies are generally greatest in the northern zone where average POC concentrations are the highest. The unusually large anomaly observed in 1998 in the equatorial region was most likely related to the El Niño event.

In Figure 7 the annual cycle of the average surface POC concentration in the entire North Atlantic region is shown. The maximum average surface POC concentration of about 85 mg m^{-3} is observed around day 120–140 (end of April/start of May). In Figure 8 we have plotted time series of the annual mean POC concentrations in the four study regions (Figures 8(*a*)–(*d*)) and the entire North Atlantic basin (Figure 8(*e*)). Data displayed in Figure 8 illustrate patterns of inter-annual variability. Estimated trends were statistically significant ($p < 0.001$ at 95% confidence level) in regions 1, 3, 4, and for the entire North Atlantic. At the basin scale average POC concentration in the North Atlantic

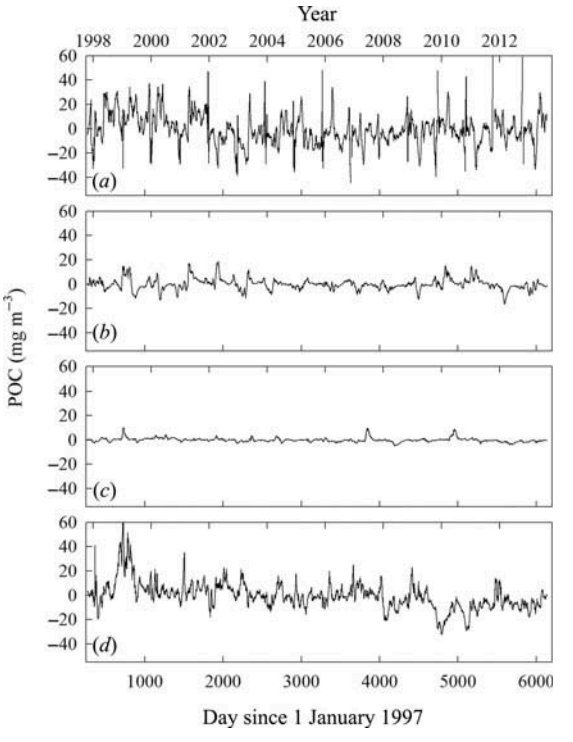

Figure 6. The 16-year (October 1997–September 2013) time series of surface POC concentration anomalies in the four geographic regions. Panels (*a*), (*b*), (*c*), and (*d*) correspond to regions 1, 2, 3, and 4, respectively.

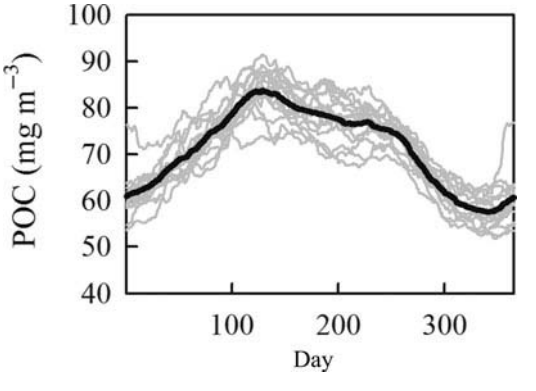

Figure 7. Time series of the POC concentration averaged over the entire area of the North Atlantic in the years 1997–2013 (grey lines) and the 16-year average annual cycle (black line).

was decreasing in the years 1997–2013 by ~0.8 mg m^{-3} per year (or ~12–13 mg m^{-3} in 16 years). Longer time series of ocean colour data are needed to explain whether this is a long-term fluctuation of POC concentration or a multiyear trend related to long-term climate change (e.g. Henson et al. 2010).

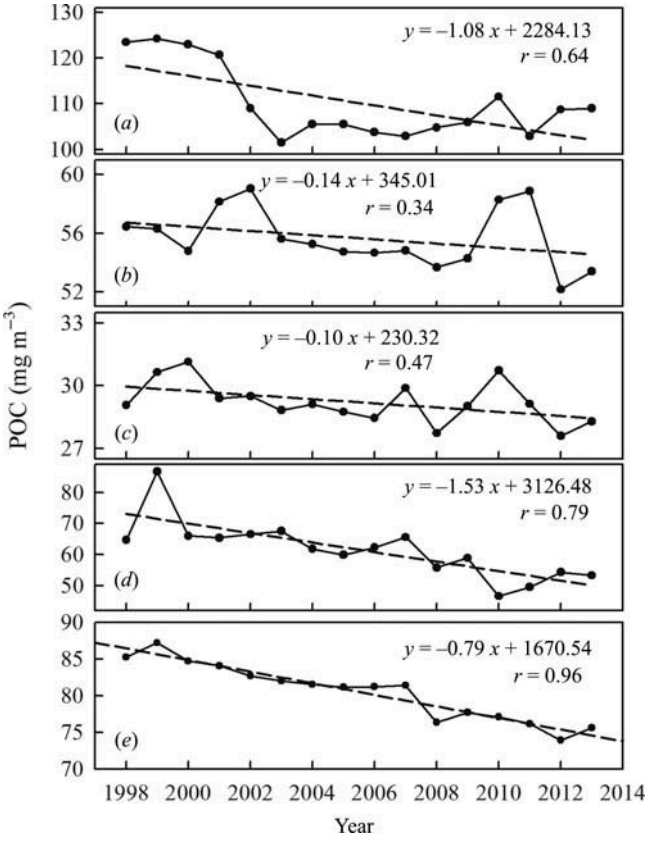

Figure 8. Time series of the annual mean POC concentrations in the four study regions (panels (*a*)–(*d*) and for the entire area of the North Atlantic (panel (*e*), see explanations in the text). Note that the vertical scale is different in each plot to better show the trends. All trends are statistically significant ($p < 0.001$ at 95% confidence level) except in region 2 (*b*).

3.2. *POC reservoirs*

In this section we assess the POC biomass present in the surface waters of the North Atlantic. As mentioned previously, such an estimate depends to a large extent on the choice of what should represent the 'oceanic surface layer'. To illustrate the differences between the POC content in various 'oceanic surface layers' we plotted in Figure 9 maps of the four estimates of the POC reservoir. All the estimates shown in Figure 9 represent the 16-year averages. These estimates include the POC biomass integrated over the optical depth (POC_{opt} shown in Figure 9(*a*)), the MLD (POC_{MLD} shown in Figure 9(*b*)), the euphotic depth (POC_{ZEU} shown in Figure 9(*c*)), and the POC biomass estimated as the greater of the POC_{MLD} and POC_{ZEU} (POC_{MAX} shown in Figure 9(*d*)). The POC_{MAX} was obtained by comparing daily POC_{MLD} and POC_{ZEU} values at every pixel. The greater of the two estimates was then used to calculate the 16-year averaged POC_{MAX}. As can be seen the lowest estimates of POC reservoir are based on the optical depth (Figure 9(*a*)). POC biomass integrated within the MLD (Figure 9(*c*)) is greater than the POC biomass integrated over the euphotic depth (Figure 9(*b*)) in the northern North Atlantic region, whereas the opposite is true in regions 3 and 4. (Note that the colour scales in Figures 9(*a*) and (*b*) are different from the scales in Figures 9(*c*) and (*d*).)

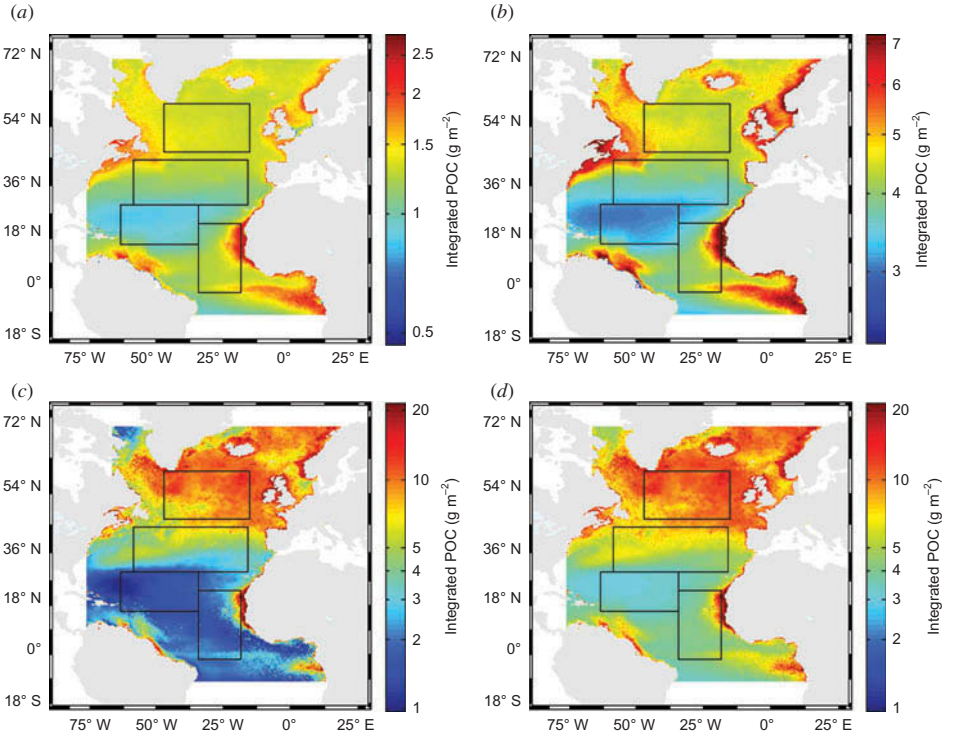

Figure 9. Maps of the 16-year averaged POC biomass integrated over the (*a*) optical depth, (*b*) euphotic depth, (*c*) mixed layer depth, and (*d*) estimate of POC_{MAX} (see explanations in the text).

In Figure 10 the annual cycles of zonally averaged z_{eu} and MLD are compared with the annual cycles of the water column integrated POC reservoirs. The MLD estimates shown in Figure 10 are based on model data obtained from the Ocean Productivity Website (web.science.oregonstate.edu/ocean.productivity/site.php). The euphotic depth estimates represent the 16-year averaged data from the NASA OceanColor Web (product zeu_Lee). Figure 10 summarizes the geographical and seasonal variability of z_{eu} and MLD. In the equatorial zone, z_{eu} is nearly double the MLD and both z_{eu} and MLD show low seasonal variability throughout the year. In contrast, the MLD in the three other regions undergoes a distinct seasonal cycle. The annual cycle of the MLD in these regions shows a summer layer shallower than 40 m from June to September. The development of this layer occurs sometime between April and June. The deepening of the MLD during the autumn seems to take a longer time (September–January). The mean MLD in the winter months is the deepest in the north, with the January–February regional 16-year averaged MLD decreasing from more than 250 m in the northern region to about 80–100 m in the oligotrophic region. In the oligotrophic region, the MLD is about 30 m during the summer, which means that the MLD is significantly less deep than z_{eu} in that season.

These regional differences in the MLD and z_{eu} are critical for understanding the control of availability of inorganic nutrients on phytoplankton biomass and PP (Cermeno et al. 2008). Typically, high latitude and temperate systems receive substantial amounts of nutrients from deep waters during the winter deepening of the MLD. In contrast, phytoplankton in the low-latitude environments, such as stratified, subtropical

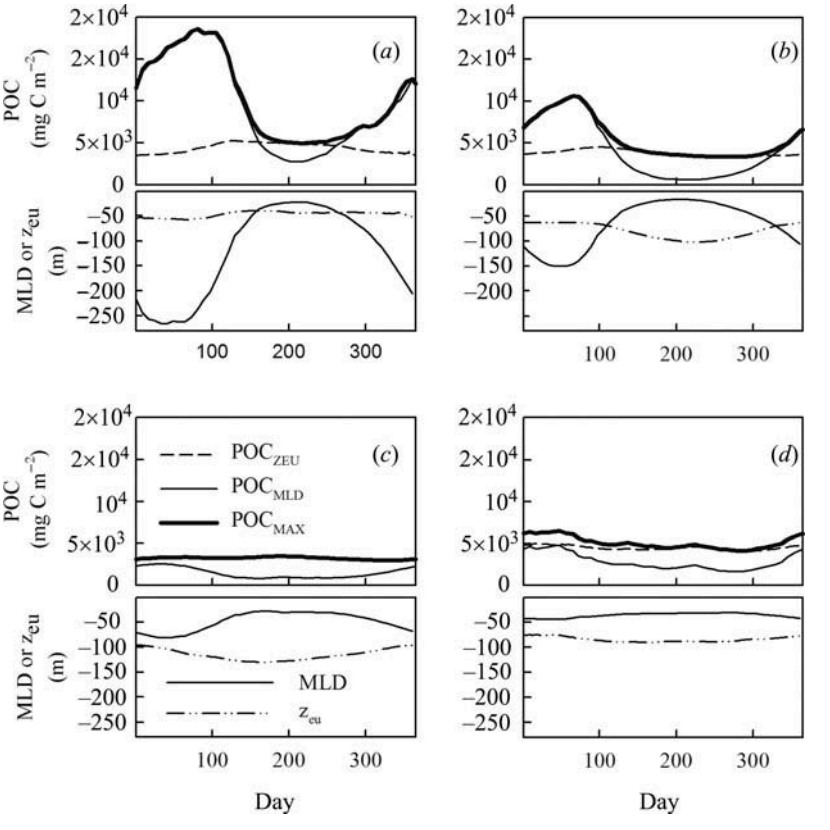

Figure 10. The 16-year averaged annual cycle of the mixed layer depth (MLD), euphotic depth (z_{eu}), POC_{ZEU}, POC_{MLD}, and POC_{MAX}. Panels (*a*), (*b*), (*c*), and (*d*) correspond to regions 1, 2, 3, and 4, respectively.

gyres, for the most part depends on local recycling and diapycnal nutrient fluxes to sustain their standing stocks. Moving from high latitudes to low latitudes in the North Atlantic, the *in situ* data show progressive deepening of the nutricline that closely parallels the depth of the euphotic layer. The PP of phytoplankton is negatively correlated with the depth of the nutricline (Cermeno et al. 2008).

The differences between z_{eu} and the MLD are significant; therefore, estimates of the POC reservoir and their spatial and temporal variability diverge considerably if we choose to use z_{eu} or the MLD as an oceanic surface layer depth. For example, because in the northern North Atlantic z_{eu} is on average shallower than the MLD, the POC reservoir integrated over z_{eu} is smaller than if it is integrated over the MLD. This is shown in Figure 10(*a*) where we plotted time series of the 16-year averaged POC integrated over the MLD (POC_{MLD}) and the 16-year average POC integrated over z_{eu} (POC_{zeu}). Regarding POC_{MLD}, it might seem somewhat surprising at first, but time series of POC_{MLD} in the northern and temperate regions (Figures 10(*a*) and (*b*)) display maximum values in the winter, despite the fact that the surface POC concentrations are much higher in the spring/summer seasons compared to the winter values. This is because MLD is much deeper in the winter than in the spring/summer. Clearly, the spring decrease of the MLD in these zones overcompensates the increase of surface POC concentrations as far as

the POC_{MLD} is concerned. In addition, POC_{MLD} does not account for the POC biomass produced in the euphotic zone below the MLD in situations when z_{eu} is deeper than the MLD. Thus, POC_{MLD} most likely underestimates the true total POC reservoir present in the surface ocean in the situation when z_{eu} is deeper than the MLD.

Note that the POC_{zeu} does not change as much as POC_{MLD} with seasons. Generally, the spring/summer increase of POC concentration is accompanied by a decrease of the z_{eu} (since water is less transparent). As can be seen, POC_{zeu} is significantly lower than POC_{MLD} in the northern and temperate zones during the winter, when the MLD reaches maximum values. Note that POC_{zeu} does not account for a large portion of POC biomass present in surface waters of the ocean. When MLD is deeper than z_{eu}, some of the biomass produced in the z_{eu} becomes redistributed through mixing below the z_{eu}. Therefore, if one wants to develop a complete POC budget in the surface waters of the ocean, it seems that POC_{zeu} in such situations is not the best choice.

We believe that a better approach to estimate the POC reservoir in the oceanic surface waters can be achieved if one uses the greater of the two estimates POC_{MLD} or POC_{zeu} (i.e. POC_{MAX}). The justification for this approach is as follows. If the MLD is greater than z_{eu}, POC biomass produced within the z_{eu} becomes redistributed within the ML by mixing. Therefore, PP reinforces changes of the POC content of the entire ML, and POC_{MLD} should be used to quantify POC reservoir. In the opposite case when the MLD is shallower than the z_{eu}, the PP affects changes of POC content of the euphotic depth and POC_{zeu} should be used to describe POC reservoir in surface waters. POC_{MLD} would not reflect these changes.

The regional differences in the POC concentration and estimates of POC reservoirs are summarized in Table 1, which shows the 16-year regional means of the POC, POC_{opt}, POC_{ZEU}, POC_{MLD}, and POC_{MAX}. The results presented in Table 1 indicate that the increase in POC biomass between the oligotrophic and the northern regions is in the order of 43%, 37%, 561%, and 221% when POC_{opt}, POC_{ZEU}, POC_{MLD}, and POC_{MAX} are considered, respectively. For comparison, averaged surface POC concentrations increase by about 280%. The results in Table 1 show that our estimate of POC_{opt} is similar to that derived by Gardner, Mishonov, and Richardson (2006) and Stramska (2009). The most important fact that we want to stress here is that if the estimate of POC standing stock is based on the MLD or z_{eu}, the POC reservoir is about 3.5 times the POC_{opt} estimate. This is due to the MLD and z_{eu} being on average significantly deeper than z_{90} (also discussed in Stramska 2009). Gardner, Mishonov, and Richardson (2006) calculated the total POC down to background levels of c_{p660} to be 2.5–5 times greater than POC_{opt}, which is in line with our more detailed calculations. Our new estimate of POC_{MLD} in the North Atlantic is about 10% higher than the similar estimate in Stramska (2009), despite the fact that the North Atlantic region boundaries in the current article include the area south of the

Table 1. Estimates of regionally averaged annual means of POC concentration and biomass in the surface waters of the North Atlantic.

Region	1	2	3	4	North Atlantic
POC concentration (mg m^{-3})	110.2	55.0	29.0	62.3	80.5
Integrated POC_{opt} (g m^{-2})	1.33	1.15	0.93	1.35	1.27
Integrated POC_{ZEU} (g m^{-2})	4.40	3.79	3.21	4.46	4.34
Integrated POC_{MLD} (g m^{-2})	9.73	4.20	1.47	2.86	4.59
POC_{MAX} (g m^{-2})	10.40	5.56	3.24	5.12	6.26

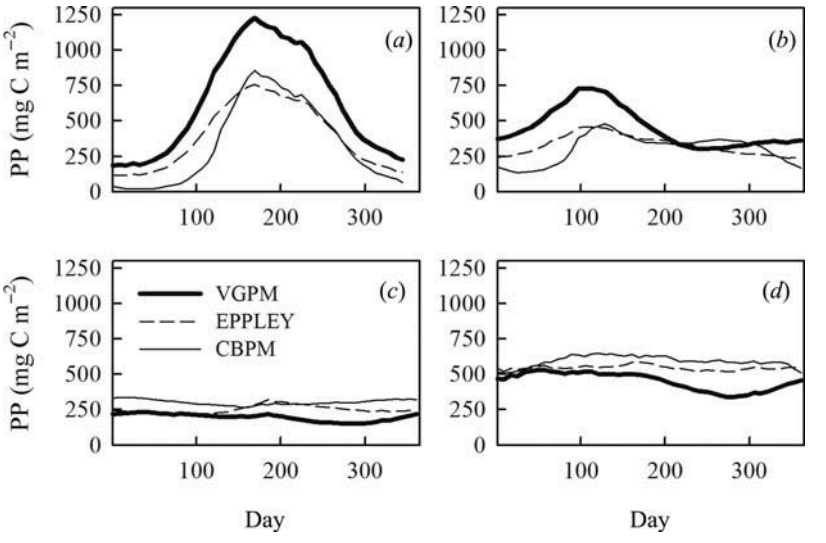

Figure 11. The 16-year averaged annual cycle of primary productivity (PP) estimated with standard VGPM, VGPM-Eppley, and CBPM models. Panels (*a*), (*b*), (*c*), and (*d*) correspond to regions 1, 2, 3, and 4, respectively.

equator (where ML is relatively shallow). The differences in both POC_{MLD} estimates are most likely because we have now used in our calculations of POC_{MLD} the MLD estimates from models with better temporal resolution than the MLD climatology data used in Stramska (2009). Finally, we note that the POC_{MAX} provides the estimate of POC reservoir in the surface waters of the North Atlantic higher by 392%, 44%, and 36% than the POC_{opt}, POC_{ZEU}, and POC_{MLD}, respectively.

The basic source of POC biomass in the surface waters of the ocean is primary production (PP). PP can be also estimated from ocean colour using PP ocean colour algorithms. The 16-year averaged PP estimates in our four study regions are displayed in Figures 11(*a*)–(*d*). These estimates are based on the standard VGPM (Behrenfeld and Falkowski 1997), the 'Eppley' version of the VGPM, and the CBPM models (Behrenfeld et al. 2005; Westberry et al. 2008). More details about these models, access to the model codes, and calculated global PP estimates are available at www.science.oregonstate.edu/ocean.productivity/index.php. Figure 11 indicates that there are significant differences between the PP estimated by different models. In particular, the largest discrepancies between the models are evident in the northern North Atlantic. The annual cycle of PP is characterized by the prominent maximum at around day 150 in the northern North Atlantic and around day 100 in the temperate region. Further south in the oligotrophic and equatorial regions, the annual cycle of PP is not well defined and the annual variability is low. It is interesting to note that the timing of the maximum PP in regions 1 and 2 happens after the maximum POC concentration is observed and when a significant decline of the POC biomass in the ML takes place.

If we consider the large-scale averages of POC content in the surface waters and assume that in such large-scale estimates the advection process can be neglected, we can use the daily estimates of POC_{MAX} and PP to calculate how much POC could have been lost from a surface layer in a given region. These estimates are based on the assumption

that a change of POC biomass in a given region over a day (ΔPOC_{MAX}) is approximately equal to the sum of gains (i.e. PP) and losses (export and recycling, POC_L).

$$\Delta POC_{MAX} = PP + POC_L. \quad (1)$$

After rearranging Equation (1) we can estimate POC losses as follows:

$$POC_L = \Delta POC_{MAX} - PP. \quad (2)$$

The annual cycles of POC_L estimated in our four study regions are displayed in Figure 12. The estimated POC_L in the northern and temperate zones exhibit a seasonal cycle with the largest POC losses (negative POC_L) during the summer. Our simple POC budget does not seem to close in the northern North Atlantic, if we assume that the PP is represented by the CBPM model. In this case the daily changes of ΔPOC_{MAX} exceed the PP estimate. This suggests that the PP might be underestimated by the CBPM model in this region in winter and early spring. The regional variability of POC losses is in agreement with recent evidence indicating that the rate of organic matter recycling is correlated with SST (Laws et al. 2000; Rivkin and Legendre 2001). Another proposed hypothesis suggests that organic matter recycling is influenced by controls related to the variability of upper ocean ecosystem structure (Lutz et al. 2007). If the supply of solar radiation and nutrients is relatively constant, environments are stable throughout the year, activities of autotrophs and heterotrophs are balanced, recycling dominates, and the fraction of production exported is minimal (oligotrophic gyres). In contrast, environments with time-varying physical conditions, solar radiation, and nutrients are characterized by 'leaky' food webs with temporally imbalanced components (e.g. high-latitude North Atlantic). In this case new production dominates and rapid autotrophic growth outpaces consumer feeding and decompositional activity (Lutz et al. 2007).

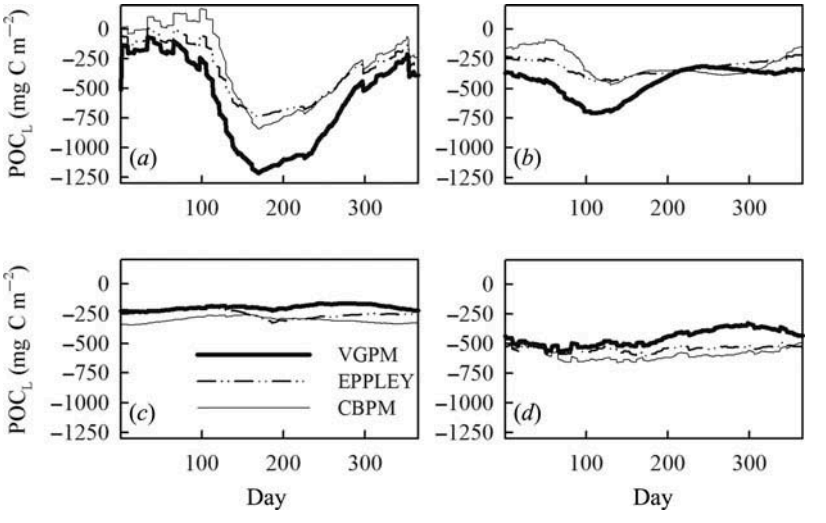

Figure 12. The 16-year averaged annual cycle of POC losses. Panels (*a*), (*b*), (*c*), and (*d*) correspond to regions 1, 2, 3, and 4, respectively.

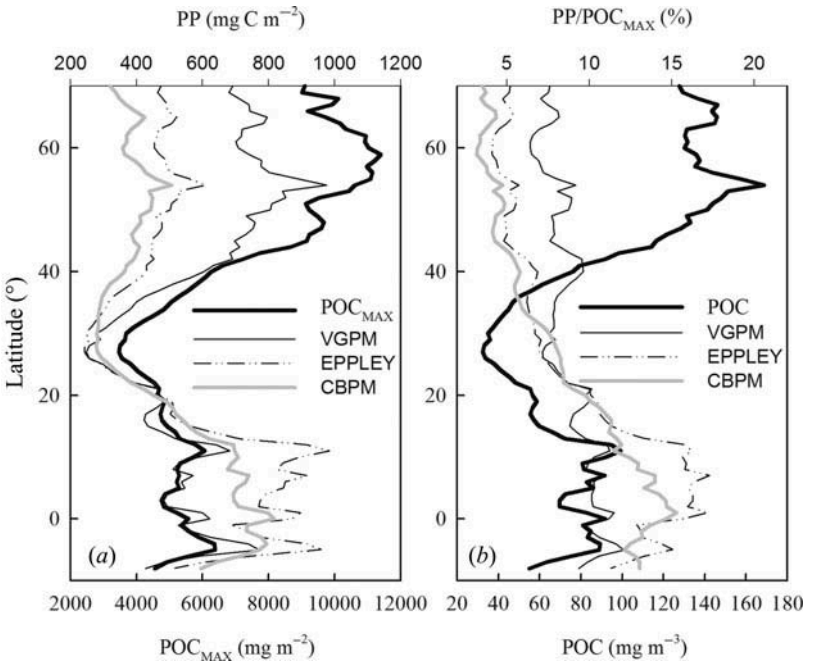

Figure 13. (*a*) Comparison of the latitudinal distribution of the POC_{MAX} with the primary productivity (PP) estimated with standard VGPM, VGPM-Eppley, and CBPM models. (*b*) Similar to (*a*), but PP expressed in % of POC_{MAX} is shown.

The characteristic latitudinal distribution of POC reservoirs and PP in the North Atlantic is summarized in Figure 13, where the 16-year averaged POC_{MAX} and PP values are plotted as a function of latitude. Characteristic features of the latitudinal POC_{MAX} distribution include the highest biomass in the range 10–12 g m^{-2} at 50–70° N, and the lowest POC_{MAX} (about 3–4 g m^{-2}) at around 30° N, increasing when moving south to about 5–6 g m^{-2} in the equatorial zone. This latitudinal distribution of POC_{MAX} is similar in different years (inter-annual variability is low). Moreover, the estimates of PP change in

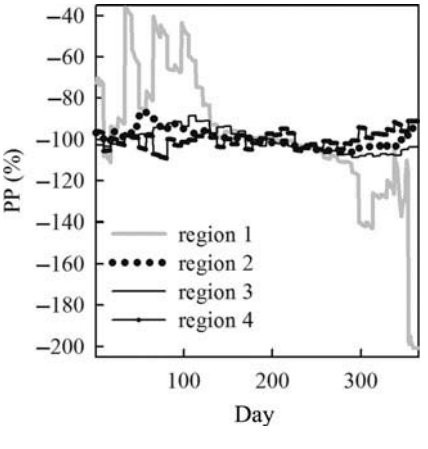

Figure 14. POC losses expressed as a percentage of the PP estimated with the VGPM model.

a characteristic way as a function of latitude, from higher values in the North, the lowest values around the 30° N, and again increasing values in the equatorial region. The VGPM model suggests that the PP reaches the highest values in the northern North Atlantic, whereas Eppley and CBPM parameterizations suggest that PP is the highest in the equatorial region. Nevertheless, the data displayed in Figure 13 indicate that the ratio of PP to POC_{MAX} in the equatorial region is about twice as big as in the northern North Atlantic. The POC losses expressed as a percentage of the PP estimated with the VGPM model show the greatest variability in region 1 (Figure 14).

In our final remarks we would like to stress that although ocean colour provides unprecedented information about large-scale oceanic processes, one needs to be aware of potential limitations. Preliminary estimates of errors in the POC algorithms in the open ocean are of the order of 30% (Stramski et al. 2008). These errors can be larger in coastal regions, but such regions contribute only a small percentage of the area included in our analysis (inland seas were excluded), and do not affect our large-scale regional estimates. Sources of such errors also include imperfections in atmospheric corrections for absorbing aerosols (e.g. Nobileau and Antoine 2005; Wang, Son, and Shi 2009) and a possible failure of the black pixel assumption in highly scattering waters (e.g. Siegel et al. 2000; Morel and Gentili 2008). Another difficulty is that ocean colour remote sensing can only provide data under clear-sky conditions; therefore, results may be biased. This problem of missing data is more severe in high latitudes due to frequent clouds and the occurrence of sea ice and polar nights; therefore, our results for the northern zone have greater uncertainty than the results for the other zones.

4. Summary and conclusions

In this article, multiyear time series of satellite data have been used to study large-scale patterns of POC variability across the North Atlantic and to quantify POC reservoirs in the surface waters. We believe that this information about POC will be of interest to Earth sciences, particularly biogeochemical and climate studies relating to the ocean carbon cycle and biological productivity. We have focused our interest on the North Atlantic, because this is a region where phytoplankton blooms are traditionally attributed an important role in the ocean carbon cycle (e.g. Longhurst and Harrison 1989; Legendre et al. 1993). It is therefore important to increase the quantitative understanding of POC reservoirs and their variability in this region.

We have shown that the characteristic spatial patterns in surface POC concentration include the highest annual mean POC concentrations in the northern North Atlantic, reaching 120 mg m^{-3}. Moving south from this region, mean annual POC concentrations decrease to minimum values of about 30 mg m^{-3} at around 30° N. Further south, POC concentrations increase in the equatorial zone to about an average of 70 mg m^{-3}. Thus, the latitudinal distribution of surface POC concentration shows the highest values in the regions where the seasonal amplitude of the MLD is large. We have shown that although the inter-annual variability in the spatial patterns of POC is quite obvious in the ocean colour imagery, time series of the large-scale average POC concentrations are quite stable, with the maximal anomalies of ±30 mg m^{-3} in the 16-year POC time series in the northern North Atlantic. The annually averaged POC concentrations show a small decreasing trend. We need longer ocean colour time series to fully understand the significance of this observation (Henson et al. 2010).

Utilizing some assumptions, we have attempted to derive quantitative information about the POC reservoir in the oceanic surface layer. Optical depth was used to derive the

POC biomass in the ocean surface waters in the literature in the past (Gardner, Mishonov, and Richardson 2006; Stramska 2009; Duforêt-Gaurier et al. 2010). Therefore, we have also estimated POC_{opt} for comparison (Table 1) and our result is similar to the earlier estimates. We have also estimated the POC biomass contained in the oceanic ML (POC_{MLD}) and euphotic layer (POC_{ZEU}). Compared with POC_{opt}, the POC_{ZEU} and POC_{MLD} estimates are considerably greater (about 3.5 times). Finally, we have proposed that if we use a simple POC_{ZEU} and POC_{MLD} estimate, we tend to underestimate the total POC biomass contained in the oceanic surface layer over the year. It seems that a more realistic annual estimate of the POC reservoir (POC_{MAX}) can be based on the choice of the greater value from the POC_{ZEU} or POC_{MLD}. We note that the POC_{MAX} provides the estimate of POC reservoir in the surface waters of the North Atlantic higher by 392%, 44%, and 36% than the POC_{opt}, POC_{ZEU}, and POC_{MLD}, respectively. Finally, the POC reservoir in the North Atlantic exhibits a clear latitudinal pattern. Moving from the oligotrophic to the northern zone, regionally averaged annual mean POC biomass increases by about 43%, 37%, 561%, and 221% when POC_{opt}, POC_{ZEU}, POC_{MLD}, and POC_{MAX} are considered, respectively.

Ocean colour remote sensing has long been recognized as a powerful means for the study of the world oceans. The application of the ocean colour POC algorithms provides a new potential to obtain long-term spatially resolved time series of POC data for detecting real trends in ocean carbon cycling. We believe that our study provides new important insights about the magnitude and variability of the oceanic POC reservoirs in the North Atlantic. Continuous long-term global monitoring of the POC in the oceans is needed to develop a better understanding of the ocean POC budget on a global scale and its climatic trends.

Acknowledgements

The author would like to thank all the people who were involved in the programmes providing free access to the data sets used in this study. The ocean colour data were made available through the NASA OceanColor Web (oceancolor.gsfc.nasa.gov/). Primary productivity and Mixed Layer Depth data were provided by the Ocean Productivity Web at the Oregon State University (www.science.oregonstate.edu/ocean.productivity/). US JGOFS data were supplied through US JGOFS Synthesis & Modeling Project (www1.whoi.edu/mzweb/syndata.html).

Funding

This work was supported by the National Science Centre (NCN) in Poland [grant number 2011/01/M/ST10/07728] “Global estimates of particulate organic carbon reservoir and export flux in the ocean based on satellite ocean colour data”.

References

Aagaard, K., J. H. Swift, and E. C. Carmack. 1985. “Thermohaline Circulation in the Arctic Mediterranean Seas.” *Journal of Geophysical Research* 90: 4833–4846. doi:10.1029/JC090iC03p04833.

Allison, D. B., D. Stramski, and B. G. Mitchell. 2010. “Empirical Ocean Color Algorithms for Estimating Particulate Organic Carbon in the Southern Ocean.” *Journal of Geophysical Research* 115: C10044. doi:10.1029/2009JC006040.

Behrenfeld, M., and E. Boss. 2014. “Resurrecting the Ecological Underpinnings of Ocean Plankton Blooms.” *Annual Review of Marine Science* 6: 167–194. doi:10.1146/annurev-marine-052913-021325.

Behrenfeld, M. J. 2010. "Abandoning Sverdrup's Critical Depth Hypothesis on Phytoplankton Blooms." *Ecology* 91: 977–989. doi:10.1890/09-1207.1.

Behrenfeld, M. J., E. Boss, D. A. Siegel, and D. M. Shea. 2005. "Carbon-based Ocean Productivity and Phytoplankton Physiology from Space." *Global Biogeochemical Cycles* 19: GB1006. doi:10.1029/2004GB002299.

Behrenfeld, M. J., and P. G. Falkowski. 1997. "Photosynthetic Rates Derived from Satellite-Based Chlorophyll Concentration." *Limnology and Oceanography* 42: 1–20. doi:10.4319/lo.1997.42.1.0001.

CAMPBELL, J. W., J. M. Blaisdell, and M. Darzi. 1995. "Level-3 SeaWiFS Data Products: Spatial and Temporal Binning Algorithms." *SeaWiFS Technical Report Series* 32: 73.

Carlson, C. A., D. A. Hansell, N. B. Nelson, D. A. Siegel, W. M. Smethie Jr., S. Khatiwala, M. M. Meyers, and E. Halewood. 2010. "Dissolved Organic Carbon Export and Subsequent Remineralization in the Mesopelagic and Bathypelagic Realms of the North Atlantic Basin." *Deep Sea Research Part II: Topical Studies in Oceanography* 57: 1433–1445. doi:10.1016/j.dsr2.2010.02.013.

Cermeno, P., S. Dutkiewicz, R. P. Harris, M. Follows, O. Schofield, and P. G. Falkowski. 2008. "The Role of Nutricline Depth in Regulating the Ocean Carbon Cycle." *Proceedings of the National Academy of Sciences of the United States of America* 105: 20344–20349. doi:10.1073/pnas.0811302106.

Clarke, G. L., G. C. Ewing, and C. J. Lorenzen. 1970. "Spectra of Backscattered Light from the Sea Obtained from Aircraft as a Measure of Chlorophyll Concentration." *Science* 167: 1119–1121. doi:10.1126/science.167.3921.1119.

Doron, M., M. Babin, A. Mangin, and O. Hembise. 2007. "Estimation of Light Penetration, and Horizontal and Vertical Visibility in Oceanic and Coastal Waters from Surface Reflectance." *Journal of Geophysical Research* 112: C06003. doi:10.1029/2006JC004007.

Duforêt-Gaurier, L., H. Loisel, D. Dessailly, K. Nordkvist, and S. Alvain. 2010. "Estimates of Particulate Organic Carbon over the Euphotic Depth from *In Situ* Measurements. Application to Satellite Data over the Global Ocean." *Deep Sea Research Part I: Oceanographic Research Papers* 57: 351–367. doi:10.1016/j.dsr.2009.12.007.

Dutkiewicz, S., M. Follows, J. Marshall, and W. W. Gregg. 2001. "Interannual Variability of Phytoplankton Abundances in the North Atlantic." *Deep Sea Research Part II: Topical Studies in Oceanography* 48: 2323–2344. doi:10.1016/S0967-0645(00)00178-8.

Franz, B. A., S. W. Bailey, P. J. Werdell, and C. R. McClain. 2007. "Sensor-Independent Approach to the Vicarious Calibration of Satellite Ocean Color Radiometry." *Applied Optics* 46: 5068–5082. doi:10.1364/AO.46.005068.

Gardner, W. D., A. V. Mishonov, and M. J. Richardson. 2006. "Global POC Concentrations from In-Situ and Satellite Data." *Deep Sea Research Part II: Topical Studies in Oceanography* 53: 718–740. doi:10.1016/j.dsr2.2006.01.029.

Gordon, H. R., and W. R. McCluney. 1975. "Estimation of the Depth of Sunlight Penetration in the Sea for Remote Sensing." *Applied Optics* 14: 413–416. doi:10.1364/AO.14.000413.

Gordon, H. R., and A. Morel. 1983. *Remote Assessment of Ocean Color for Interpretation of Satellite Visible Imagery – A Review. Lecture Notes on Coastal and Estuarine Studies,* 114 pp. New York: Springer-Verlag.

Henson, S. A., J. L. Sarmiento, J. P. Dunne, L. Bopp, I. Lima, S. C. Doney, J. John, and C. Beaulieu. 2010. "Detection of Anthropogenic Climate Change in Satellite Records of Ocean Chlorophyll and Productivity." *Biogeosciences* 7: 621–640. doi:10.5194/bg-7-621-2010.

Houghton, R. A. 2007. "Balancing the Global Carbon Budget." *Annual Review of Earth and Planetary Sciences* 35: 313–347. doi:10.1146/annurev.earth.35.031306.140057.

Kraus, E. B., R. Bleck, and H. P. Hanson. 1988. "The Inclusion of a Surface Mixed Layer in a Large-scale Circulation Model." In *Small Scale Turbulence and Mixing in the Ocean*, edited by J. C. J. Nihoul and B. M. Jamart, 51–62. Amsterdam: Elsevier.

Laws, E. A., P. G. Falkowski, W. O. Smith, H. Ducklow, and J. J. McCarthy. 2000. "Temperature Effects on Export Production in the Open Ocean." *Global Biogeochemical Cycles* 14: 1231–1246. doi:10.1029/1999GB001229.

Lee, Z.-P., M. Darecki, K. L. Carder, C. O. Davis, D. Stramski, and W. J. Rhea. 2005. "Diffuse Attenuation Coefficient of Downwelling Irradiance: An Evaluation of Remote Sensing Methods." *Journal of Geophysical Research* 110: C02017. doi:10.1029/2004JC002573.

Lee, Z.-P., K. P. Du, and R. Arnone. 2005. "A Model for the Diffuse Attenuation Coefficient of Downwelling Irradiance." *Journal of Geophysical Research* 110: C02016. doi:10.1029/2004JC002275.

Lee, Z.-P., A. Weidemann, J. Kindle, R. Arnone, K. L. Carder, and C. Davis. 2007. "Euphotic Zone Depth: Its Derivation and Implication to Ocean-Color Remote Sensing." *Journal of Geophysical Research* 112: C03009. doi:10.1029/2006JC003802.

Legendre, L., M. Gosselin, H.-J. Hirche, G. Kattner, and G. Rosenberg. 1993. "Environmental Control and Potential Fate of Size-Fractionated Phytoplankton Production in the Greenland Sea (75 °N)." *Marine Ecology Progress Series* 98: 297–313. doi:10.3354/meps098297.

Loisel, H., E. Bosc, D. Stramski, K. Oubelkheir, and P.-Y. Deschamps. 2001. "Seasonal Variability of the Backscattering Coefficient in the Mediterranean Sea Based on Satellite SeaWiFS Imagery." *Geophysical Research Letters* 28: 4203–4206. doi:10.1029/2001GL013863.

Loisel, H., J.-M. Nicolas, P.-Y. Deschapms, and R. Frouin. 2002. "Seasonal and Inter-Annual Variability of Particulate Organic Matter in the Global Ocean." *Geophysical Research Letters* 29 (24): 2196. doi:10.1029/2002GL015948.

Longhurst, A. R. 1998. *Ecological Geography of the Sea*. New York: Academic Press.

Longhurst, A. R., and W. G. Harrison. 1989. "The Biological Pump: Profiles of Plankton Production and Consumption in the Upper Ocean." *Progress in Oceanography* 22: 47–123. doi:10.1016/0079-6611(89)90010-4.

Lorbacher, K., D. Dommenget, P. P. Niiler, and A. Köhl. 2006. "Ocean Mixed Layer Depth: A Subsurface Proxy of Ocean-Atmosphere Variability." *Journal of Geophysical Research* 111: C07010. doi:10.1029/2003JC002157.

Lutz, M. J., K. Caldeira, R. B. Dunbar, and M. J. Behrenfeld. 2007. "Seasonal Rhythms of Net Primary Production and Particulate Organic Carbon Flux to Depth Describe the Efficiency of Biological Pump in the Global Ocean." *Journal of Geophysical Research* 112: C10011. doi:10.1029/2006JC003706.

McClain, C. R., G. C. Feldman, and S. B. Hooker. 2004. "An Overview of the SeaWiFS Project and Strategies for Producing a Climate Research Quality Global Ocean Bio-Optical Time Series." *Deep Sea Research Part II: Topical Studies in Oceanography* 51: 5–42. doi:10.1016/j.dsr2.2003.11.001.

Menzel, D. W., and J. H. Ryther. 1961. "Annual Variations in Primary Production of the Sargasso Sea off Bermuda." *Deep Sea Research (1953)* 7: 282–288. doi:10.1016/0146-6313(61)90046-6.

Mishonov, A. V., W. D. Gardner, and M. J. Richardson. 2003. "Remote Sensing and Surface POC Concentration in the South Atlantic." *Deep Sea Research Part II: Topical Studies in Oceanography* 50: 2997–3015. doi:10.1016/j.dsr2.2003.07.007.

Morel, A. 1988. "Optical Modeling of the Upper Ocean in Relation to its Biogenous Matter Content (Case I Waters)." *Journal of Geophysical Research* 93: 10749–10768. doi:10.1029/JC093iC09p10749.

Morel, A., and B. Gentili. 2008. "Practical Application of the "Turbid Water" Flag in Ocean Color Imagery: Interference with Sun-glint Contaminated Pixels in Open Ocean." *Remote Sensing of Environment* 112: 934–938. doi:10.1016/j.rse.2007.07.009.

Morel, A., and L. Prieur. 1977. "Analysis of Variations in Ocean Color." *Limnology and Oceanography* 22: 709–722. doi:10.4319/lo.1977.22.4.0709.

Niiler, P. P., and E. B. Kraus. 1977. "One-dimensional Models of the Upper Ocean." In *Modelling and Predictions of the Upper Layers of the Ocean*, edited by E. B. Kraus, 143–172. Oxford: Pergamon.

Nobileau, D., and D. Antoine. 2005. "Detection of Blue-Absorbing Aerosols Using near Infrared and Visible (Ocean Color) Remote Sensing Observations." *Remote Sensing of Environment* 95: 368–387. doi:10.1016/j.rse.2004.12.020.

O'Reilly, J. E., S. Maritorena, B. G. Mitchell, D. A. Siegel, K. L. Carder, S. A. Garver, M. Kahru, and C. R. McClain. 1998. "Ocean Color Chlorophyll Algorithms for SeaWiFS." *Journal of Geophysical Research* 103: 24937–24953. doi:10.1029/98JC02160.

O'Reilly, J. E., S. Maritorena, D. A. Siegel, M. C. O'Brien, D. Toole, B. G. Mitchell, and M. Kahru et al. 2000. "Ocean Color Chlorophyll a Algorithms for SeaWiFS, OC2 and OC4: Version 4." *NASA Technical Memo, 2000-206892* 11: 9–27.

Pabi, S., and K. R. Arrigo. 2006. "Satellite Estimation of Marine Particulate Carbon in Waters Dominated by Different Phytoplankton Taxa." *Journal of Geophysical Research* 110: C10018. doi:10.1029/2005JC003137.

Rivkin, R. B., and L. Legendre. 2001. "Biogenic Carbon Cycling in the Upper Ocean: Effects of Microbial Respiration." *Science* 291: 2398–2400. doi:10.1126/science.291.5512.2398.

Siegel, D. A., M. J. Behrenfeld, S. Maritorena, C. R. McClain, D. Antoine, S. W. Bailey, P. S. Bontempi, E. S. Boss, H. M. Dierssen, S. C. Doney, R. E. Eplee, R. H. Evans, G. C. Feldman, E. Fields, B. A. Franz, N. A. Kuring, C. Mengelt, N. B. Nelson, F. S. Patt, W. D. Robinson, J. L. Sarmiento, C. M. Swan, P. J. Werdell, T. K. Westberry, J. G. Wilding, and J. A. Yoder. 2013. "Regional to Global Assessments of Phytoplankton Dynamics from the SeaWiFS Mission." *Remote Sensing of Environment* 135: 77–91. doi:10.1016/j.rse.2013.03.025.

Siegel, D. A., M. Wang, S. Maritorena, and W. Robinson. 2000. "Atmospheric Correction of Satellite Ocean Color Imagery: The Black Pixel Assumption." *Applied Optics* 39: 3582–2591. doi:10.1364/AO.39.003582.

Son, Y. B., W. D. Gardner, A. V. Mishonov, and M. J. Richardson. 2009. "Multispectral Remote Sensing Algorithms for Particulate Organic Carbon (POC): The Gulf of Mexico." *Remote Sensing of Environment* 113: 50–61. doi:10.1016/j.rse.2008.08.011.

Stramska, M. 2009. "Particulate Organic Carbon in the Global Ocean Derived from SeaWiFS Ocean Color." *Deep Sea Research I*. doi:10.1016/j.dsr.2009.04.009

Stramska, M., and T. Dickey. 1993. "Phytoplankton Bloom and the Vertical Thermal Structure of the Upper Ocean." *Journal of Marine Research* 51: 819–842. doi:10.1357/0022240933223918.

Stramska, M., and T. Dickey. 1994. "Modeling Phytoplankton Dynamics in the Northeast Atlantic during the Initiation of the Spring Bloom." *Journal of Geophysical Research* 99: 10241–10253. doi:10.1029/93JC03378.

Stramska, M., and D. Stramski. 2005a. "Variability of Particulate Organic Carbon Concentration in the North Polar Atlantic Based on Ocean Color Observations with Sea-viewing Wide Field-of-view Sensor (SeaWiFS)." *Journal of Geophysical Research* 110: C10018. doi:10.1029/2004JC002762.

Stramska, M., and D. Stramski. 2005b. "Effects of a Nonuniform Vertical Profile of Chlorophyll Concentration on Remote-Sensing Reflectance of the Ocean." *Applied Optics* 44: 1735–1747. doi:10.1364/AO.44.001735.

Stramski, D., R. A. Reynolds, M. Babin, S. Kaczmarek, M. R. Lewis, R. Röttgers, A. Sciandra, M. Stramska, M. S. Twardowski, B. A. Franz, and H. Claustre. 2008. "Relationships between the Surface Concentration of Particulate Organic Carbon and Optical Properties in the Eastern South Pacific and Eastern Atlantic Oceans." *Biogeosciences* 5: 171–201. doi:10.5194/bg-5-171-2008. www.biogeosciences.net/5/171/2008/.

Stramski, D., R. A. Reynolds, M. Kahru, and B. G. Mitchell. 1999. "Estimation of Particulate Organic Carbon in the Ocean from Satellite Remote Sensing." *Science* 285: 239–242. doi:10.1126/science.285.5425.239.

Sverdrup, H. U. 1953. "On Conditions for the Vernal Blooming of Phytoplankton." *ICES Journal of Marine Science* 18: 287–295. doi:10.1093/icesjms/18.3.287.

Townsend, D. W., M. D. Keller, M. E. Sieracki, and S. G. Ackleson. 1992. "Spring Phytoplankton Blooms in the Absence of Vertical Water Column Stratification." *Nature* 360: 59–62. doi:10.1038/360059a0.

Wang, M., S. Son, and W. Shi. 2009. "Evaluation of MODIS SWIR and NIR-SWIR Atmospheric Correction Algorithms Using SeaBASS Data." *Remote Sensing of Environment* 113: 635–644. doi:10.1016/j.rse.2008.11.005.

Westberry, T., M. J. Behrenfeld, D. A. Siegel, and E. Boss. 2008. "Carbon-Based Primary Productivity Modeling with Vertically Resolved Photoacclimation." *Global Biogeochemical Cycles* 22: GB2024. doi:10.1029/2007GB003078.

Yoder, J. A., and M. A. Kennelly. 2006. "What Have We Learned about Ocean Variability from Satellite Ocean Color Imagers?" *Oceanography* 19 (1): 152–171. doi:10.5670/oceanog.2006.98.